atmosphere

MDPI

Article

Modified Transmission Line Model with a Current Attenuation Function Derived from the Lightning Radiation Field—MTLD Model

Vernon Cooray [1,*], Marcos Rubinstein [2] and Farhad Rachidi [3]

[1] Department of Electrical Engineering, Uppsala University, 752 37 Uppsala, Sweden
[2] HEIG-VD, University of Applied Sciences and Arts Western Switzerland, 1401 Yverdon-les-Bains, Switzerland; Marcos.Rubinstein@heig-vd.ch
[3] Electromagnetic Compatibility Laboratory, Swiss Federal Institute of Technology (EPFL), 1015 Lausanne, Switzerland; Farhad.Rachidi@epfl.ch
* Correspondence: vernon.cooray@angstrom.uu.se

Abstract: In return strokes, the parameters that can be measured are the channel base current and the return stroke speed. For this reason, many return stroke models have been developed with these two parameters, among others, as inputs. Here, we concentrate on the current propagation type engineering return stroke models where the return stroke is represented by a current pulse propagating upwards along the leader channel. In the current propagation type return stroke models, in addition to the channel base current and the return stroke speed, the way in which the return stroke current attenuates along the return stroke channel is specified as an input parameter. The goal of this paper is to show that, within the confines of current propagation type models, once the channel base current and the return stroke speed are known, the measured radiation field can be used to evaluate how the return stroke current attenuates along the channel. After giving the mathematics necessary for this inverse transformation, the procedure is illustrated by extracting the current attenuation curve from the typical wave shape of the return stroke current and from the distant radiation field of subsequent return strokes. The derived attenuation curve is used to evaluate both the subsequent and first return stroke electromagnetic fields at different distances. It is shown that all the experimentally observed features can be reproduced by the derived attenuation curve, except for the subsidiary peak and long zero-crossing times. In order to obtain electromagnetic fields of subsequent return strokes that are in agreement with measurements, one has to incorporate the current dispersion into the model. In the case of first return strokes, both current dispersion and reduction in return stroke speed with height are needed to obtain the desired features.

Keywords: lightning; return strokes; radiation fields; current attenuation; remote sensing; modified transmission line models; MTL models; MTLD model

Citation: Cooray, V.; Rubinstein, M.; Rachidi, F. Modified Transmission Line Model with a Current Attenuation Function Derived from the Lightning Radiation Field—MTLD Model. *Atmosphere* **2021**, *12*, 249. https://doi.org/10.3390/atmos12020249

Academic Editor: Martino Marisaldi

Received: 30 December 2020
Accepted: 8 February 2021
Published: 13 February 2021

1. Introduction

Features of electromagnetic fields from lightning return strokes are needed at different distances in studies related to the interaction of these electromagnetic fields with both the Earth's upper atmosphere and man-made electrical structures [1–3]. Moreover, these fields at different distances are also important in understanding the way in which they are attenuated and dispersed as they propagate along rough and finitely conducting grounds [4–6]. These studies require electromagnetic fields of return strokes at different distances with different time resolutions depending on the requirements of the study. Since measuring electromagnetic fields from return strokes at several distances simultaneously is a difficult task, researchers have employed return stroke models to calculate these electromagnetic fields.

Return stroke models can be divided into different categories depending on the basic principles used in constructing them. They can be divided into physical models,

transmission line models, antenna models, electromagnetic models and engineering models [7]. Engineering models are the simplest, yet they are highly successful in predicting electromagnetic fields of return strokes at different distances from the lightning channel. Engineering return stroke models specify either directly or indirectly how the return stroke current attenuates and disperses along the return stroke channel. These models can be divided into three subtypes, namely, the current propagation, current generation, and current dissipation models [7]. Here, we will focus on current propagation type return stroke models in which the upward propagation characteristics of the return stroke current injected at the channel base are specified. The engineering return stroke models that belong to this category are the transmission line model (TL model) and its modifications [8–10]. These modifications of the transmission line model are known as the modified transmission line models (MTL models). Frequently used MTL models are the Modified Transmission Line Model with Exponential Decay (MTLE) [9,11] and the Modified Transmission Line Model with Linear Decay (MTLL) models [10]. There are several other MTL models with different attenuation functions and they are described in [12]. Before proceeding further, let us consider the goals of an engineering return stroke model.

According to the information available at present, during the return stroke, a current pulse is initiated at ground level and it propagates along the leader channel while undergoing attenuation and dispersion. The information necessary to extract how the return stroke current varies along the channel is embedded in the resulting electromagnetic fields. These models utilize various expressions for the current attenuation and dispersion to figure out which of these expressions would provide a best fit to the electromagnetic fields generated by lightning. At first glance, this may appear as a curve fitting procedure. However, this is the best tool available for the researchers to extract information concerning how the return stroke current disperses and attenuates as it propagates along the channel. The MTL models are best suited for this purpose because the current attenuation function and the current dispersion function can be specified directly and independently in these models. If the selected features of the model with input parameters constrained by the measured return stroke current and the measured return stroke speed provide a best fit to the electromagnetic fields measured at several distances (distant, intermediate and close), one can accept with confidence the model features as a good representation of the way in which the return stroke current disperses and attenuates as it propagates along the channel. In this exercise, there is no need to restrict the number of model parameters because the way in which the current behaves as it propagates upward could be very complicated and this complex change in the current waveform with height cannot be described by only a few model parameters. However, it is important to stress that what is gained by engineering models is the information concerning *how* the return stroke current attenuates and disperses along the channel and not *why* the current is changing in that manner. Answering the latter is a task for the physicists who are engaged in creating physics-based return stroke models. However, once the attenuation function and the way in which the current dispersion are correctly identified, they will provide a complete description of the temporal and spatial variation of the return stroke current. Thus, the creators of engineering models attempt to extract, sometimes making reasonable guesses, the information necessary for the physicists to decipher the mechanism of the return stroke. Note that creating a theory by guessing is a valid procedure, according to Richard Feynman [13], provided that the predictions of the theory agree with experiment. Let us now consider the engineering return stroke models which are pertinent to the current study.

In the TL model, the return stroke is simulated by an injected current at the channel base that travels up along the return stroke channel with constant speed and without dispersion or attenuation. In the MTLE model, it is assumed that the current decays exponentially with height and, in the MTLL model, it is assumed that the current decays linearly as a function of height. Both these models assume zero dispersion of the return stroke current with height. The current at any given height in these models can be specified by the equation

$$\begin{aligned} i(t,z) &= i_b(t - z/v)A(z) \;\; t \geq z/v \\ i(t,z) &= 0 \qquad t < z/v \end{aligned} \tag{1}$$

In the above equation, $A(z)$ is a parameter that specifies the way in which the return stroke current amplitude decreases with height z, $i_b(t)$ is the channel base current and v is the speed of propagation of the return stroke front. Equations (2)–(4) given below specify the function $A(z)$ for the TL, MTLE and MTLL models, respectively.

$$A(z) = 1.0 \tag{2}$$

$$A(z) = \exp(-z/\lambda) \tag{3}$$

$$A(z) = (1 - z/H) \tag{4}$$

In the above expressions, λ is the decay height constant and H is the height of the return stroke channel.

Observe that the MTL models require as inputs the channel base current and the return stroke speed in addition to the third input parameter that specifies the way in which the current attenuates with height. The first two parameters can be measured in practice, but the third parameter has to be assumed. Moreover, another parameter that can be measured is the distant radiation fields associated with the return strokes. Once the return stroke speed and the current attenuation function are specified, one can derive the channel base current from the measured radiation field [14]. However, existing measurement techniques do not allow the direct measurement of the way in which the current attenuates along the channel and, for this reason, different functions are used in MTL models to describe this variation. The goal of this paper is to illustrate how to remove the arbitrary assumptions involved in the specification of the attenuation of the current along the return stroke channel in these models by extracting this information directly from the measurable parameters. As we will show in the next section, all the information necessary to extract the current attenuation function is available in the distant radiation field provided that the return stroke speed and the channel base current, both of which are measurable parameters, are given. One should point out here that several attempts have been previously made to extract the return stroke current and the attenuation function from the measured fields. Delfino et al. [15] and Andreotti et al. [16] developed frequency domain numerical techniques to extract both the current and the attenuation function from the close electric and magnetic fields of return strokes. Willett et al. [17] and Izadi et al. [18] developed time domain techniques to extract the return stroke current and the attenuation function. Actually, these time domain techniques do not solve the inverse problem but compare the measured electromagnetic fields with the ones obtained using an assumed current and/or attenuation function and change these parameters until a good fit is found for the measurements.

2. Extracting the Current Attenuation Function from the Distant Radiation Field

Let us refer to Figure 1 for the geometry relevant to the calculations. The lightning channel is assumed to be straight and vertical and it is located above a perfectly conducting ground plane. The positive z-axis of the coordinate system is directed perpendicularly out of the ground. The electric field at any given distance at ground level has only a component directed along the z-axis and, based on the dipole technique, it is given by [19].

$$\begin{aligned} E_z(t) = \tfrac{1}{2\pi\varepsilon_0} \int_0^{L(t-D/c)} \tfrac{2-3\sin^2\theta}{R^3} dz \int_{t-z/v_{av}-R/c}^{t} i(z,\tau)d\tau \\ + \tfrac{1}{2\pi\varepsilon_0} \int_0^{L(t-D/c)} \tfrac{2-3\sin^2\theta}{cR^2} i(z,t-R/c)dz - \tfrac{1}{2\pi\varepsilon_0} \int_0^{L(t-D/c)} \tfrac{\sin^2\theta}{c^2R} \tfrac{\partial i(z,t-R/c)}{\partial t} dz \text{ with } t > D/c \end{aligned} \tag{5}$$

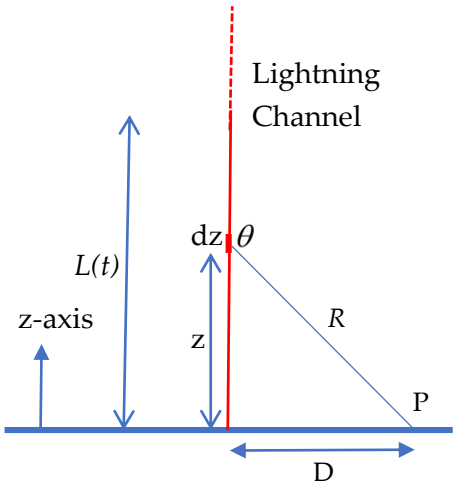

Figure 1. Geometry relevant to the calculation of the electromagnetic fields from a return stroke. In the diagram, $L(t)$ is the return stroke front as seen by an observer at P.

In the previous equation, c is the speed of light in free space, $i(z,t)$ is the current at height z along the return stroke channel and $L(t)$ is the length of the return stroke channel at time t as seen by an observer located at the field point. Note the difference between H used in Equation (4) and $L(t)$ in (5). In Equation (4), H is the final length of the return stroke channel, whereas $L(t)$ in Equation (5) is the extending height of the return stroke front as seen by the observer located at P at time t. Thus, $L(t)$ is a length that increases with time. Note that, since $L(t)$ is the length of the channel as seen by the observer, it is a nonlinear function of t and not simply the product of the constant speed times t. The rest of the parameters are defined in Figure 1. If the distance to the point of observation is large, then only the term proportional to $1/R$ in Equation (5), known as the radiation field, is dominant and the expression for the electric field reduces to

$$E_z(t) = -\frac{1}{2\pi\varepsilon_0}\int_0^{L(t-D/c)} \frac{\sin^2\theta}{c^2 R}\frac{\partial i(z,t-R/c)}{\partial t}dz \tag{6}$$

Further, if the distance to the point of observation is much larger than the dimension of the source (i.e., $D >> L$), then the radiation field reduces to

$$E_z(t) = -\frac{1}{2\pi\varepsilon_0 c^2 D}\int_0^{L(t-D/c)} \frac{\partial i(z,t-D/c)}{\partial t}dz \tag{7}$$

Let us now assume that we have measurements pertinent to the channel base current and the return stroke speed. Then, using the MTL model, the current at any height can be written as

$$i(t,z) = i_b(t - z/v_{av})A(z) \tag{8}$$

In the above equation, v_{av}, which is a function of z, is the average speed of the return stroke from ground level to height z. This is given by

$$v_{av} = z/\int_0^z \frac{dz}{v(z)} \tag{9}$$

with $v(z)$ representing the variation of the return stroke speed with height. Substituting the expression given in Equation (8) for the current into Equation (7), we obtain

$$E_z(t) = -\frac{1}{2\pi\varepsilon_0 c^2 D}\int_0^{L(t-D/c)} A(z)\frac{\partial i_b(t-D/c-z/v_{av})}{\partial t}dz \tag{10}$$

Let us divide the channel into elements Δz in such a way that it is the length traversed by the return stroke front during each time step Δt as observed from the point at which the radiation field is measured. Since the distance to the point of observation is much larger than the length L, and if the speed of propagation is constant, say v, then $\Delta z = v\Delta t$. If the speed is changing, then Δz varies with time in such a way that the length traveled during Δt when the return stroke front is at height z is $\Delta z = v(z)\Delta t$. Thus, the return stroke field at distance D can be written as the summation (with $K = -1/2\pi\varepsilon_0 c^2 D$).

$$\begin{aligned} E_z(D/c + n\Delta t) = K\left(\tfrac{\partial i_b(t)}{\partial t}\right)_{n\Delta t} A_1\Delta z_1 + K\left(\tfrac{\partial i_b(t)}{\partial t}\right)_{(n-1)\Delta t} A_2\Delta z_2 \\ + K\left(\tfrac{\partial i_b(t)}{\partial t}\right)_{(n-2)\Delta t} A_3\Delta z_3 \ldots\ldots\ldots + K\left(\tfrac{\partial i_b(t)}{\partial t}\right)_{\Delta t} A_n\Delta z_n \end{aligned} \tag{11}$$

This can be written as

$$E_z(D/c + n\Delta t) = K\sum_{m=1}^{n}\left(\frac{\partial i_b(t)}{\partial t}\right)_{m\Delta t} A_{n-m+1}\Delta z_{n-m+1} \tag{12}$$

Note that the first term of this equation is the contribution to the field from the first element (bottom element) of the return stroke channel. From this equation, one can extract the function A sequentially as follows. Consider the case with n = 1. Substituting $\Delta z_1 = v_1\Delta t$, where v_1 is the speed of propagation of the current along the first element, we obtain (note that z_1 = 0)

$$E_z(D/c + \Delta t) = K\left(\frac{\partial i_b(t)}{\partial t}\right)_{\Delta t} A_1 v_1\Delta t \tag{13}$$

Since the channel base current and the return stroke speed as a function of height are known, the only unknown parameter is the value of A_1, which can be extracted from the above equation. Now consider the case with n = 2. In this case

$$E_z(D/c + 2\Delta t) = K\left(\frac{\partial i_b(t)}{\partial t}\right)_{2\Delta t} A_1 v_1\Delta t + K\left(\frac{\partial i_b(t)}{\partial t}\right)_{\Delta t} A_2 v_2\Delta t \tag{14}$$

The only unknown in the above equation is A_2 which can be extracted from it. In this way, the identity of the function $A(z)$ can be extracted sequentially. This procedure is illustrated in the next section using the MTLE and MTLL models.

3. Examples of the Extracted Current Attenuation

In order to test the validity of the extracted current attenuation function, let us consider the MTLE and MTLL models. The channel base current of both first and subsequent return strokes will be represented by Heidler's functions [20].

$$i_c(t) = i_{01}\frac{(t/\tau_{11})^2}{(t/\tau_{11})^2 + 1}e^{-t/\tau_{12}} + i_{02}\frac{(t/\tau_{21})^2}{(t/\tau_{21})^2 + 1}e^{-t/\tau_{22}} \tag{15}$$

The parameters corresponding to the channel base current of subsequent return strokes are: i_{01} = 13.618 kA, i_{02} = 8.268 kA, τ_{11} = 0.05 μs, τ_{12} = 2.5 μs, τ_{21} = 2.0 μs and τ_{22} = 100 μs. First strokes were represented only by the first term of Equation (15) with i_{01} = 30.551 kA, τ_{11} = 0.09 μs and τ_{12} = 95 μs. Now, we will use the radiation fields of subsequent return

strokes calculated at 500 km using the MTLE and MTLL models to extract the attenuation function. In the MTLE model, a value of λ = 2000 m and, in the MTLL model, H = 7500 m are selected as typical parameters [9–11]. The return stroke speed is kept constant at 1.5×10^8 m/s. The extracted current attenuation functions from the radiation fields of the two models using the equations given in the previous section are shown in Figure 2 (black dashed lines) together with the actual attenuation function used in the calculations (red solid lines). Observe that the extracted curves are nearly identical to the actual ones. This demonstrates that the attenuation curve can be extracted from the measured radiation fields if the channel base current and the return stroke speed are given.

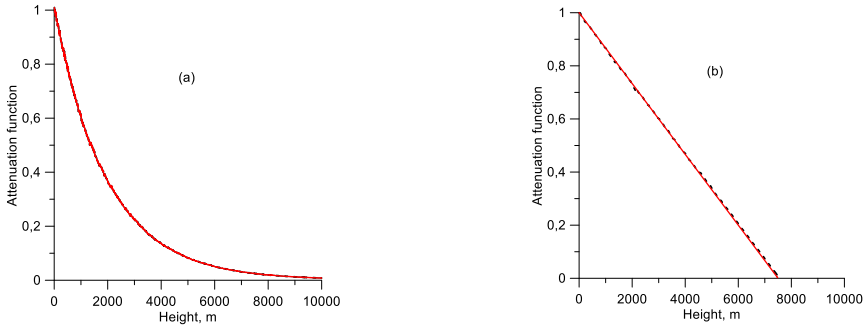

Figure 2. Attenuation curve extracted from the calculated radiation field. (**a**) MTLE model. (**b**) MTLL model. The attenuation curves are extracted from the radiation fields that would be present at a 500 km distance over perfectly conducting and flat ground.

It is important to point out that for an accurate estimation of the attenuation curve, one needs to utilize the pure radiation field. In the examples shown in Figure 2 we have used the radiation field that would be present at 500 km over flat ground. This large distance validates the assumption that the electric field is pure radiation. However, as the distance to the lightning flash becomes smaller, the contribution to the electric field from the static and induction terms increases and this can cause errors in the extracted attenuation function. In order to study this effect, we have extracted the attenuation function from electric fields calculated at different distances using the expression given in Equation (12). The results obtained for both the MTLL and MTLE models are shown in Figure 3. Note that the derived attenuation function deviates from the real one (curve a) as the distance to the lightning channel becomes shorter. Since the contribution to the electric field by the static term increases with time, for a given distance, the error in the attenuation function is larger at larger heights than at the smaller heights.

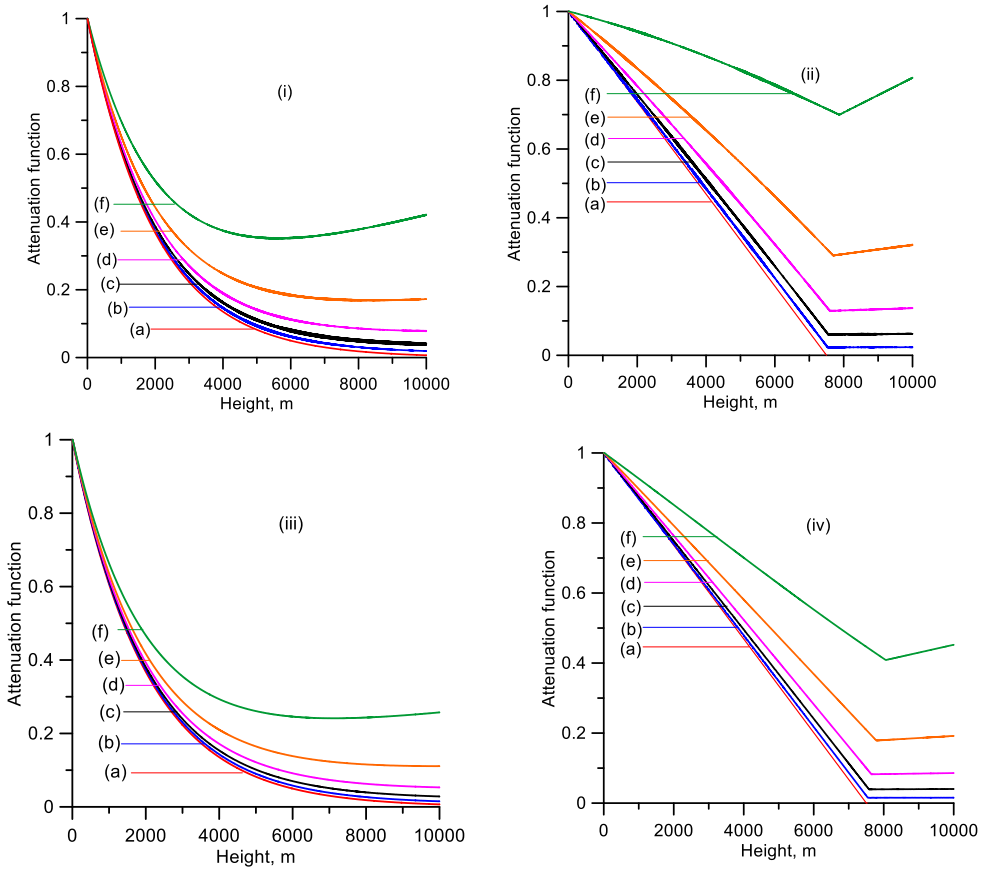

Figure 3. Attenuation functions derived from the electric field at different distances. (**i**) MTLE model, first strokes; (**ii**) MTLL model, first strokes; (**iii**) MTLE model, subsequent strokes; (**iv**) MTLL model, subsequent strokes. (a) Pure radiation, (b) 500 km, (c) 200 km, (d) 100 km, (e) 50 km, (f) 25 km.

4. Current Attenuation Function Extracted from Typical Radiation and Current Waveforms of Subsequent Return Strokes

We used the following procedure to construct an example of a typical radiation field pertinent to subsequent return strokes in the tropics and to obtain the corresponding attenuation function. First, a set of reference points outlining the general shape of the radiation field with a peak amplitude of about 3.5 V/m (the peak value pertinent to the TL model for a 12 kA peak current and return stroke speed equal to 1.5×10^8 m/s) is constructed. The reference points were based on the field measurements carried out in Sri Lanka and Malaysia [21,22] (data from Malaysia were provided to the authors by Dr. Ridual Ahmed). The initial rising part of the constructed radiation field is matched to the initial rising part of the radiation field (up to the initial peak) calculated using the transmission line model using the average subsequent return stroke current given by Equation (15) and a uniform speed of 1.5×10^8 m/s. This condition is based on the assumption that the return stroke can be represented by a current pulse that moves upwards with constant speed. Since the current attenuation and change in speed can be neglected for very small times (or in channel elements close to the ground), the above is a reasonable and also a necessary assumption to be made. In the next step, the current attenuation function pertinent to the constructed radiation field is obtained. The resulting current attenuation function is represented by a polynomial (using a standard plotting routine) and the coefficients of the polynomial are changed until a best fit (based on a least square optimization procedure) to the reference points of the radiation field is obtained. It is important to point out that in order to obtain a smooth attenuation function, in the trial-and-error procedure we have used, the reference points we started with had to be changed somewhat to obtain a good

fit. However, during this procedure, the main features of the radiation field, such as the risetime and zero-crossing time, were not changed. The radiation field and the attenuation function that resulted from this exercise are shown in Figure 4. The risetime of the radiation field is located at around 0.5–0.6 μs and the peak value normalized to 100 km is around 3.5 V/m. The mean zero-crossing time of the radiation field is 47 μs, which is a good fit for the measurements conducted in Sri Lanka. The amplitude of the radiation field decays to about 40% of its peak value in about 15 μs and the amplitude of the opposite overshoot is about 0.13 of the initial peak value. Both these features agree with the ones in the measured waveforms.

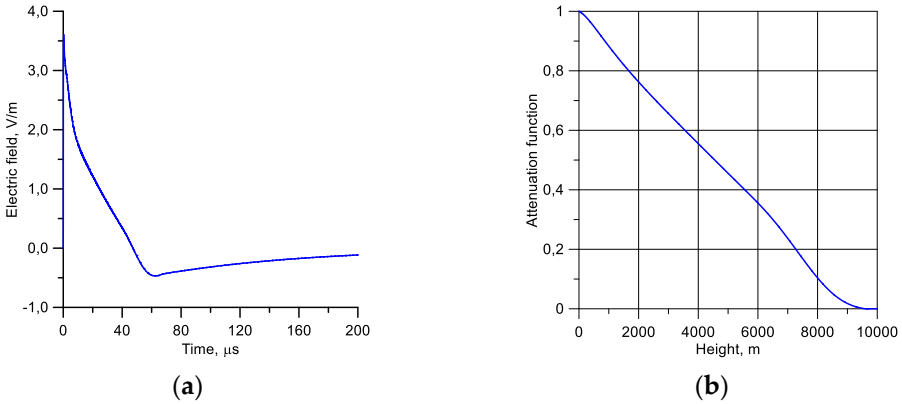

Figure 4. (**a**) Radiation field assumed to represent the subsequent return stroke radiation fields in the tropics. (**b**) Current attenuation function pertinent to the radiation field shown in Figure 4a.

It is important to point out that in the experimental data pertinent to return stroke radiation fields, there is a shoulder or a small peak (subsidiary peak) in the decaying part of the waveform [23,24]. For reasons to be described later, this feature is not included when constructing the radiation field.

Observe that the derived attenuation function depend on the radiation field used as an input, and it will change from one return stroke radiation field to another. The attenuation function derived here can be used to evaluate the fields of subsequent return strokes at different distances in tropical regions. The main change that takes place in return strokes when one moves from one geographical region to another is the change in the length of the channel. Note that the height at which the derived attenuation function goes to zero is close to 10 km. However, the height to the charge centers, and hence the return stroke channel length, could be smaller in temperate regions. Later, we will show how the derived attenuation function can be modified to take into account the different channel lengths.

In the next section, we will use the derived attenuation function in the MTL type model to calculate the electromagnetic fields at different distances. For the reasons given above, note that the fields to be presented present the typical features pertinent to the subsequent return strokes in the tropics.

5. MTLD Model—Subsequent Return Strokes

In this section, we will use the attenuation function derived in the previous section in an MTL-type model to calculate the electromagnetic fields generated by subsequent return strokes. Since the model differs from the other MTL models in that the attenuation function is derived from the radiation field, we will call this model Modified Transmission Line Model with Derived Attenuation Function (MTLD).

The electric and magnetic fields obtained from the MTLD model are compared with the ones obtained from the other two commonly used MTL models (i.e., MTLE and MTLL) in Figures 5 and 6, respectively. In this calculation, the channel base current pertinent to subsequent return strokes and a uniform return stroke speed equal to 1.5×10^8 m/s

were used in all the models. In the MTLE model, λ = 2000 m and, in the MTLL model, H = 10,000 m.

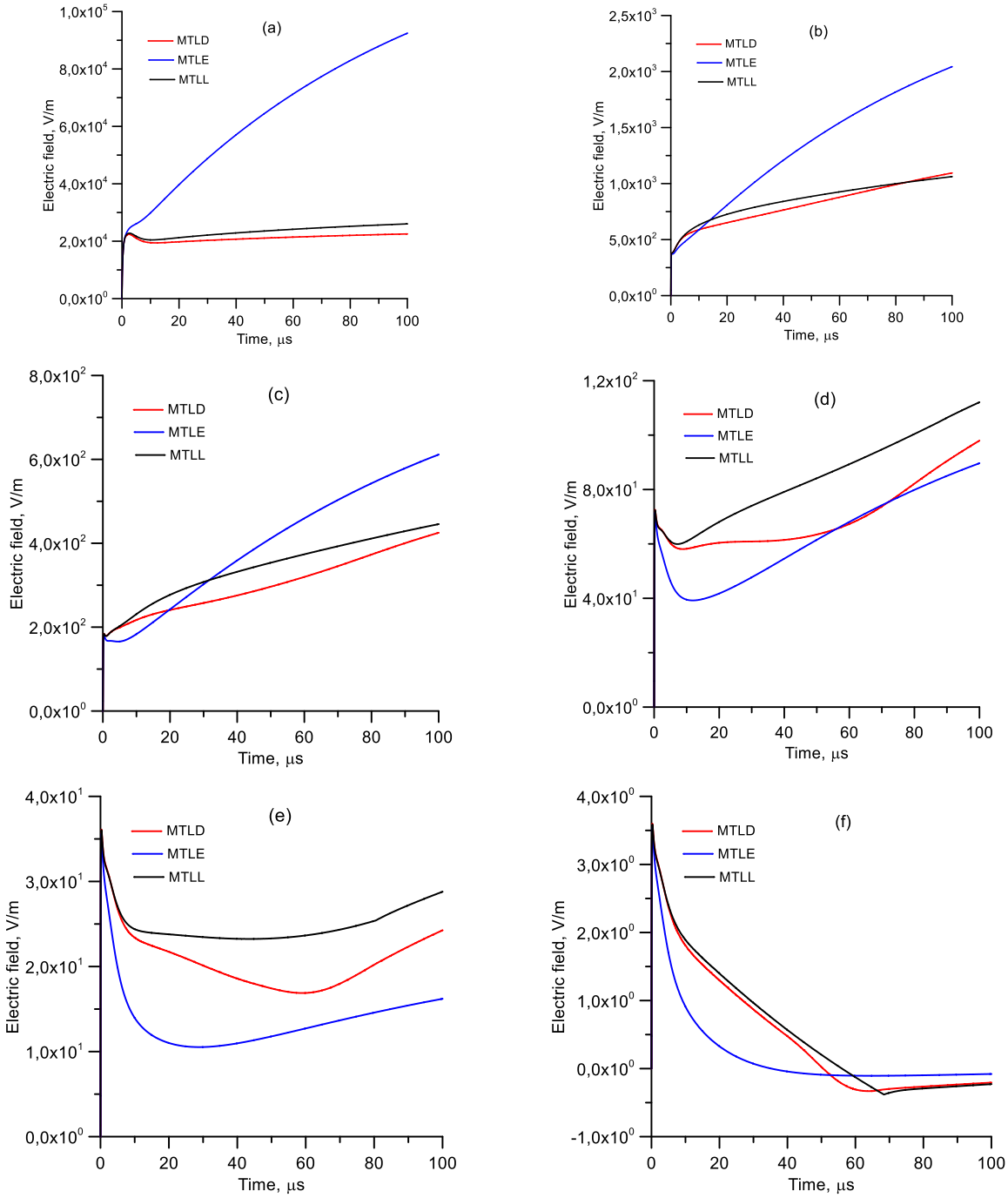

Figure 5. Electric fields of subsequent return strokes at different distances as predicted by the MTLD, MTLE and MTLL models. (**a**) 50 m, (**b**) 1 km, (**c**) 2 km, (**d**) 5 km, (**e**) 10 km and (**f**) 100 km. In the MTLE model, λ = 2 km and, in the MTLL model, H = 10 km are used as model parameters. The return stroke speed is assumed to be constant and equal to 1.5×10^8 m/s.

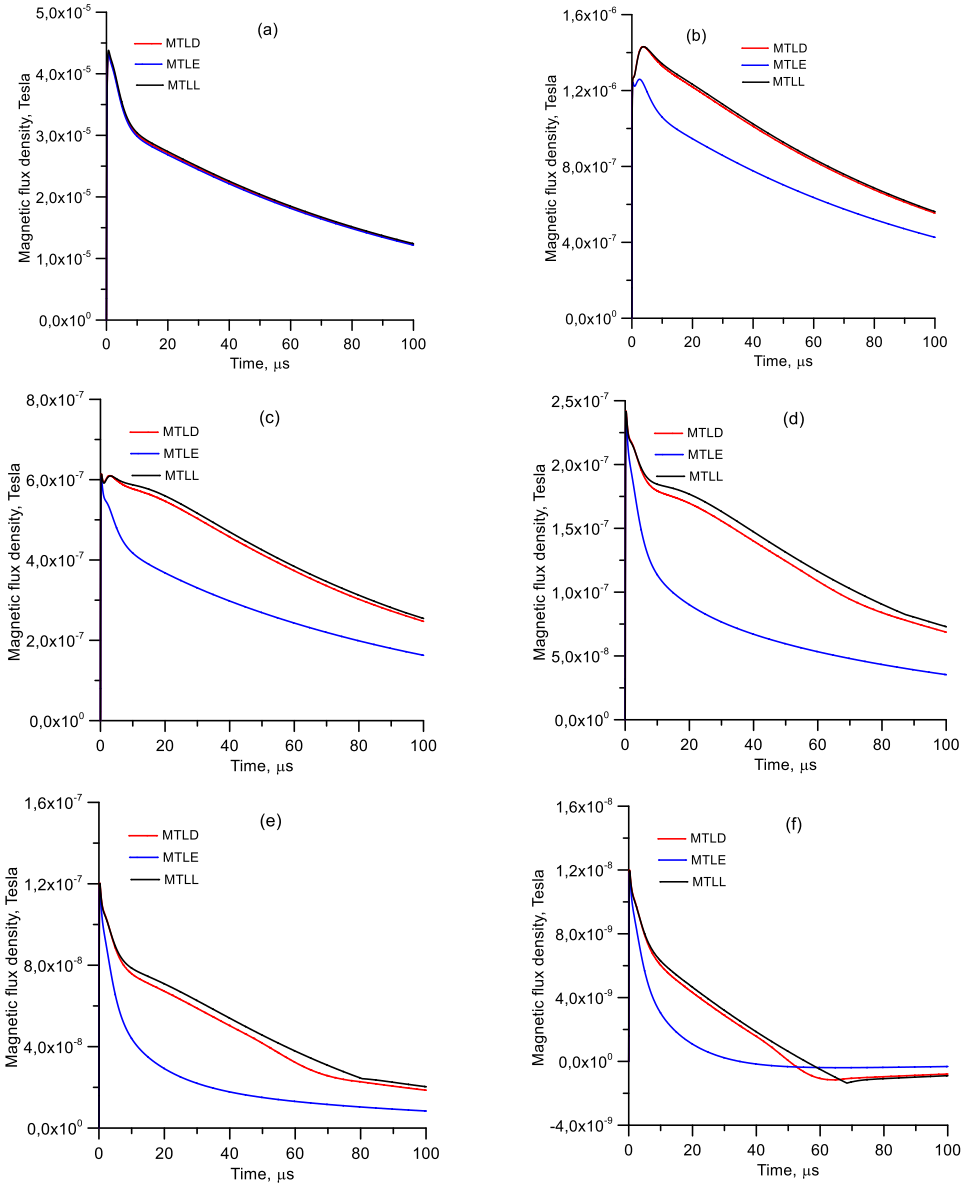

Figure 6. Magnetic fields of subsequent return strokes at different distances as predicted by the MTLD, MTLE and MTLL models. (**a**) 50 m, (**b**) 1 km, (**c**) 2 km, (**d**) 5 km, (**e**) 10 km and (**f**) 100 km. In the MTLE model, λ = 2.0 km and, in the MTLL model, H = 10 km are used as model parameters. The return stroke speed is assumed to be constant and equal to 1.5×10^8 m/s.

Note that there are similarities and differences in the close and distant electromagnetic fields calculated using these different models. Observe that experimental data on the features of electromagnetic fields from lightning within 100 m are available for the subsequent return strokes in triggered lightning flashes. This information shows that the close field saturates within a few tens of microseconds from the beginning of the return stroke. The close field of the subsequent return stroke obtained using the MTLD is in agreement with this observation. Observe also that none of the models could generate a significant hump in the close (i.e., 1 km to 10 km) magnetic fields which is a significant feature in the measured fields [24]. However, the magnetic fields of the MTLD and MTLL model display a slight hump in the magnetic field in the distant range of 5 km to 10 km.

The results presented above are based on the attenuation functions derived from a typical radiation field constructed with temporal features and zero-crossing times pertinent to tropical regions. The derived attenuation function can be used in engineering studies

which require electromagnetic fields at different distances in those latitudes. The way to modify the current attenuation function to obtain electric fields pertinent to other geographical regions where channel lengths and hence zero-crossing times of radiation fields are lower is provided in Section 8.

6. MTL Models and the Subsidiary Peak in the Radiation Fields of Subsequent Return Strokes

As mentioned earlier, a subsidiary peak in the radiation fields and the hump in the close magnetic fields are characteristic features of subsequent return stroke radiation fields [23,24]. However, our calculations show that a subsequent return stroke radiation field with a subsidiary peak in combination with the standard subsequent return stroke current waveform of Equation (15) will give rise to an attenuation function which is physically unreasonable. We will come back to this point again later. In order to get a physically reasonable attenuation function from a radiation field with a subsidiary peak, one has to utilize a channel base current waveform that also has a subsidiary peak. However, according to the experimental data available, the measured subsequent return stroke currents only display subsidiary peaks occasionally [25,26]. The reason for this puzzling problem and a possible solution are described below.

In general, the amplitude and the shape of the radiation field are determined by the amplitude and wave shape of the channel base current, how this current attenuates and disperses as it propagates along the channel, the spatial variation of the return stroke speed and current enhancements that may occur in the channel caused by the branch components [23,27]. Subsequent return strokes are typically free of branches. Thus, any enhancement of the radiation field (i.e., subsidiary peak) is caused either by a temporal increase in the return stroke speed or a change in the return stroke current along the channel. Some works have suggested a possible increase in the return stroke speed along the channel at the initiation of the return stroke [28–30]. Although our analysis shows that such an increase could generate an initial peak immediately after the return stroke, it cannot generate a broader subsidiary peak around 10–20 μs as in the measured radiation fields unless the return stroke speed starts to increase after the return stroke front has traveled a distance of around 1 km or so. However, we cannot find any physical reason for such a transient increase in the return stroke speed after the return stroke front has already traversed several hundreds of meters or so of the channel, especially when, as mentioned, the return stroke channel is free of branches. More experimental data are needed before a conclusion can be made on the role of return stroke speed, if any, on the occurrence of subsidiary peaks in the return stroke radiation fields. Here, we assume that the subsidiary peak of the subsequent radiation field is caused by the variation of return stroke current shape along the channel. As we will show later, the enhancement in the electric field cannot be caused by a change in the current attenuation because such a change will lead to physically unacceptable charge deposition along the return stroke channel. Thus, we are left with the current dispersion as the possible reason for the subsidiary peak in the radiation field.

Cooray and Orville [31] studied the effect of various return stroke parameters on the return stroke radiation fields. They observed that the current dispersion along the channel could give rise to a radiation field with a subsidiary peak. By current dispersion, we mean the variation of the time domain current waveshape caused by the different speeds of propagation and attenuation of various frequency components as they propagate along the lightning channel. However, in order to produce a subsidiary peak, the dispersion of the current should be such that the current risetime increases initially with height but, as the height increases further, the risetime should reach a more or less threshold value. A return stroke where the current risetime increases monotonically could not generate a subsidiary peak. Based on this observation, we have incorporated a dispersion function that generates the abovementioned features in the MTLD model. The dispersion function is defined with respect to the propagation of a Dirac delta function along the channel. In the absence of any information concerning the way in which the current is dispersed along the

return stroke channel, we have utilized an exponential function to represent the dispersion. The exponential function is somewhat similar to the dispersion of an electromagnetic field represented by a Dirac delta function over a finitely conducting ground [32]. According to the dispersion formula introduced into the model, a delta function at ground level will be distorted as it propagates along the channel according to the formula

$$R_\delta(t,z) = \frac{e^{-t/t_r(z)}}{t_r(z)} \tag{16}$$

Observe that the time integral of $R_\delta(t,z)$ is equal to unity, a criterion that is necessary to make sure that there is no charge deposition along the channel due to current dispersion. The parameter $t_r(z)$ is given by

$$t_r(z) = t_{r0}(1 - e^{-z^2/\lambda_r^2}) \tag{17}$$

This dispersion formula also shows that a step current pulse at ground level will change with height according to the expression

$$R_H(t,z) = 1 - e^{-t/t_r(z)} \tag{18}$$

Observe that the risetime of the step current pulse increases initially but it will be clamped to a fixed value as the height increases beyond about λ_r. As we will show later, this clamping of the risetime is a necessary feature in the current dispersion in order to generate a subsidiary peak. Such a scenario is also physically reasonable for the following reason. As the current propagates upward, the removal of the high frequencies from the current waveform increases its risetime. This is because the propagation of a pulse in a lossy medium results mainly in an attenuation of its high-frequency components. As the risetime increases, it becomes less and less sensitive to further removal of high frequencies and the risetime of the current waveform reaches more or less a steady value. The actual dispersed current at any level can be obtained by convoluting the channel base current with the delta response function given by Equation (16). Alternatively, it can also be obtained from the step response given in Equation (18) using Duhammel's theorem.

Figure 7 shows several examples of the radiation field calculated at 100 km for different values of t_{r0} and λ_r. Observe that radiation fields similar to the typical examples given by Weidman and Krider [23] are obtained for t_{r0} in the range of 2–5 μs and λ_r (the parameter that defines the risetime of the current in Equation (17)) in the range of 500–1000 m. Observe also that a monotonically increasing risetime in the dispersion formula could not generate a subsidiary peak. It is important to point out that we have selected the parameter z^2/λ_r^2 in the exponential of Equation (18) instead of z/λ_r, which will also give rise to a clamping of the risetime with height. However, our calculations show that the latter would give rise to a rather significant reduction in the initial peak of the radiation field due to the rapid increase in the risetime of the current close to the bottom of the channel. This makes the relationship between the initial part of the channel base current and the radiation field differ somewhat from the transmission line model. However, the validity of the transmission line model for the initial part of the radiation field is an assumption that we have made in the construction of the MTLD model.

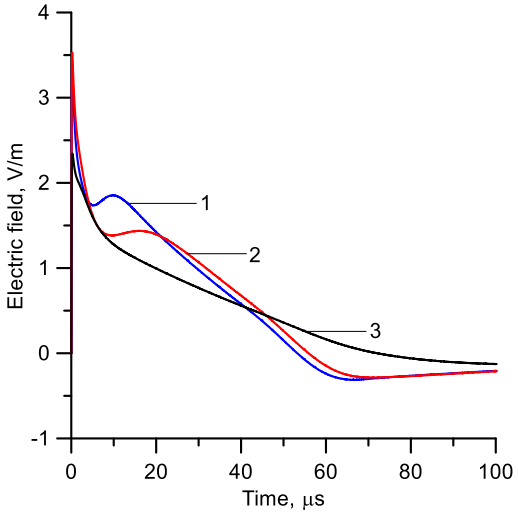

Figure 7. Radiation field at 100 km for different forms of the dispersion function. (1) $t_r(z) = 2.5 \times 10^{-6}[1 - e^{-(z/500)^2}]$, (2) $t_r(z) = 5.0 \times 10^{-6}[1 - e^{-(z/1000)^2}]$, (3) $t_r(z) = 5.0 \times 10^{-6}z/1000.0$. In these equations, z is the height along the return stroke channel.

The electromagnetic fields calculated at different distances incorporating the current dispersion into the MTLD model are shown in Figures 8 and 9. In this calculation, we have selected t_{r0} = 2.5 μs and λ_r = 500 m. Observe that the calculated fields display all the features of the measured subsequent return stroke fields. For example, the electric field at 50 m saturates within a few microseconds, the tail of the electric field around 1 to 5 km shows a ramp-like increase and the corresponding magnetic fields display a prominent hump. Moreover, the radiation fields cross the zero line and display the characteristic subsidiary peak. These features show that even though the introduction of current dispersion makes the model slightly more complex, it compensates for this by generating electromagnetic fields with features in good agreement with experimental observations. Furthermore, the current dispersion is a feature that is always present in actual return strokes, as demonstrated by Jordan and Uman [33] and Mack and Rust [34] using optical radiation, and incorporating this into the return stroke current is a necessity in modeling the return strokes. It is important to point out that inferences concerning both the return stroke speed and the current attenuation are based on the properties of the optical radiation produced by the lightning return stroke. This in turn assumes that at any given height, the return stroke current waveform faithfully follows the waveform of the optical radiation generated at that height at least during the first few microseconds from the onset of the optical radiation. Some evidence that this could be the case is provided from both laboratory and field experiments [35,36].

At the beginning of this section, we mentioned that a radiation field exhibiting a subsidiary peak is not compatible with a pure MTL-type model. Let us now expand on this statement. First, observe that in calculating the radiation field shown by curve 1 in Figure 7, we used the current attenuation function shown in Figure 4b while incorporating current dispersion into the model. Let us now use this radiation field to extract the apparent attenuation function using Equation (12) but without taking into account the presence of dispersion. The resulting attenuation function is shown in Figure 10. Observe that this attenuation function contains a subsidiary peak. According to this attenuation function, there will be a gradual enhancement of the return stroke current at higher levels along the return stroke channel. However, since the return stroke current is transporting positive charge upwards, such a current enhancement can only be possible if the corona sheath supplies a positive charge to the core of the return stroke. This in turn requires the deposition of negative charge along the channel where the current enhancement is taking place. We believe that this scenario is physically unreasonable. The second point is that had we used the current attenuation curve shown in Figure 10 in an MTL-type

model without dispersion, the resulting electromagnetic fields at different distances would not have displayed the characteristic features pertinent to the measured fields. For these reasons, we conclude that for uniform or monotonically decreasing return stroke speeds, subsequent return stroke radiation fields with subsidiary peaks are not compatible with MTL-type models that do not incorporate current dispersion. Of course, one can make them compatible with MTL models without current dispersion by selecting a channel base current waveform with a subsidiary peak, but, as mentioned earlier, in general, the measured channel base currents in general do not display such subsidiary peaks.

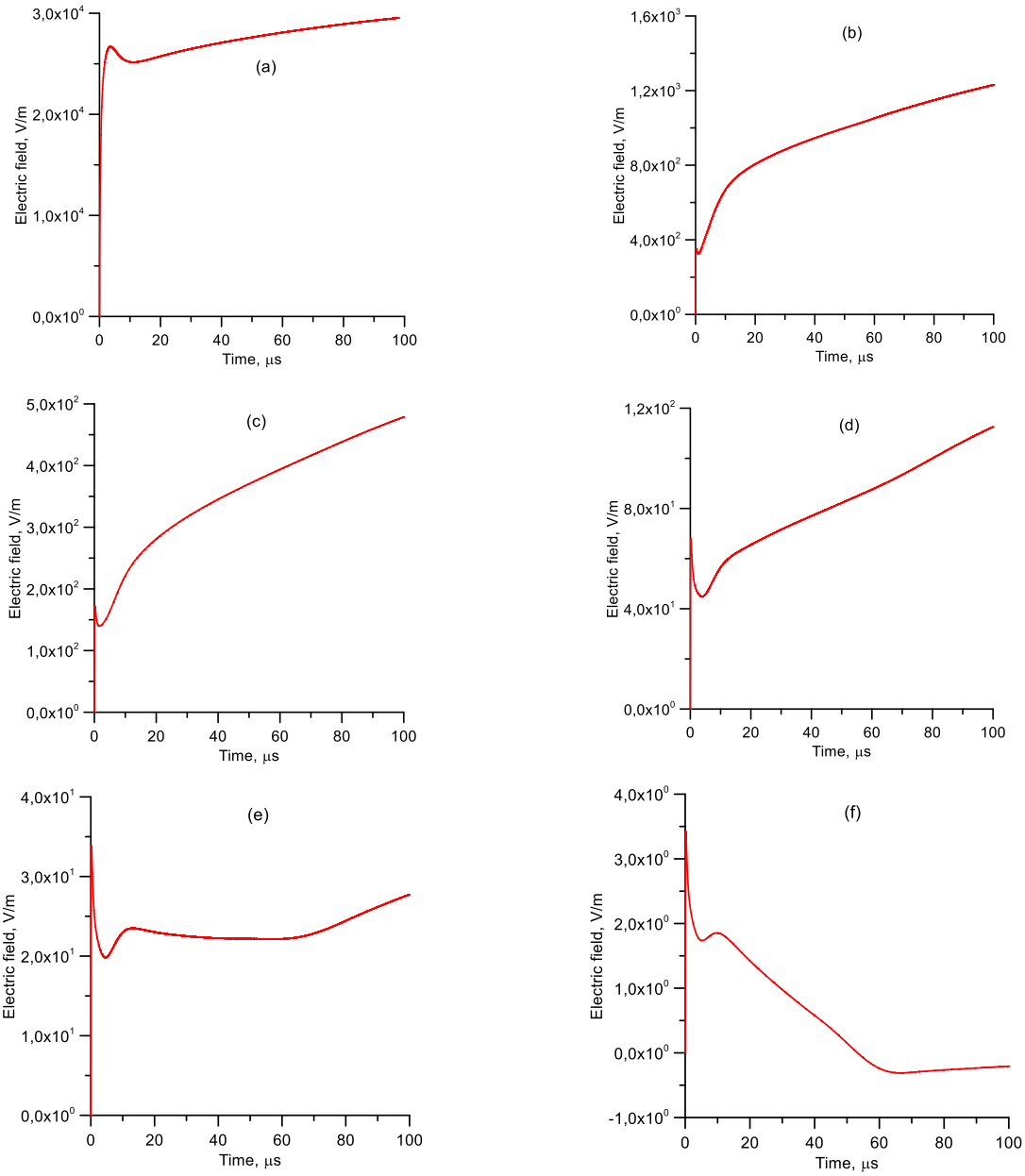

Figure 8. Electric field of subsequent return strokes at different distances as predicted by the MTLD model that incorporates current dispersion. (**a**) 50 m, (**b**) 1 km, (**c**) 2 km, (**d**) 5 km, (**e**) 10 km and (**f**) 100 km. The return stroke speed is assumed to be constant and equal to 1.5×10^8 m/s.

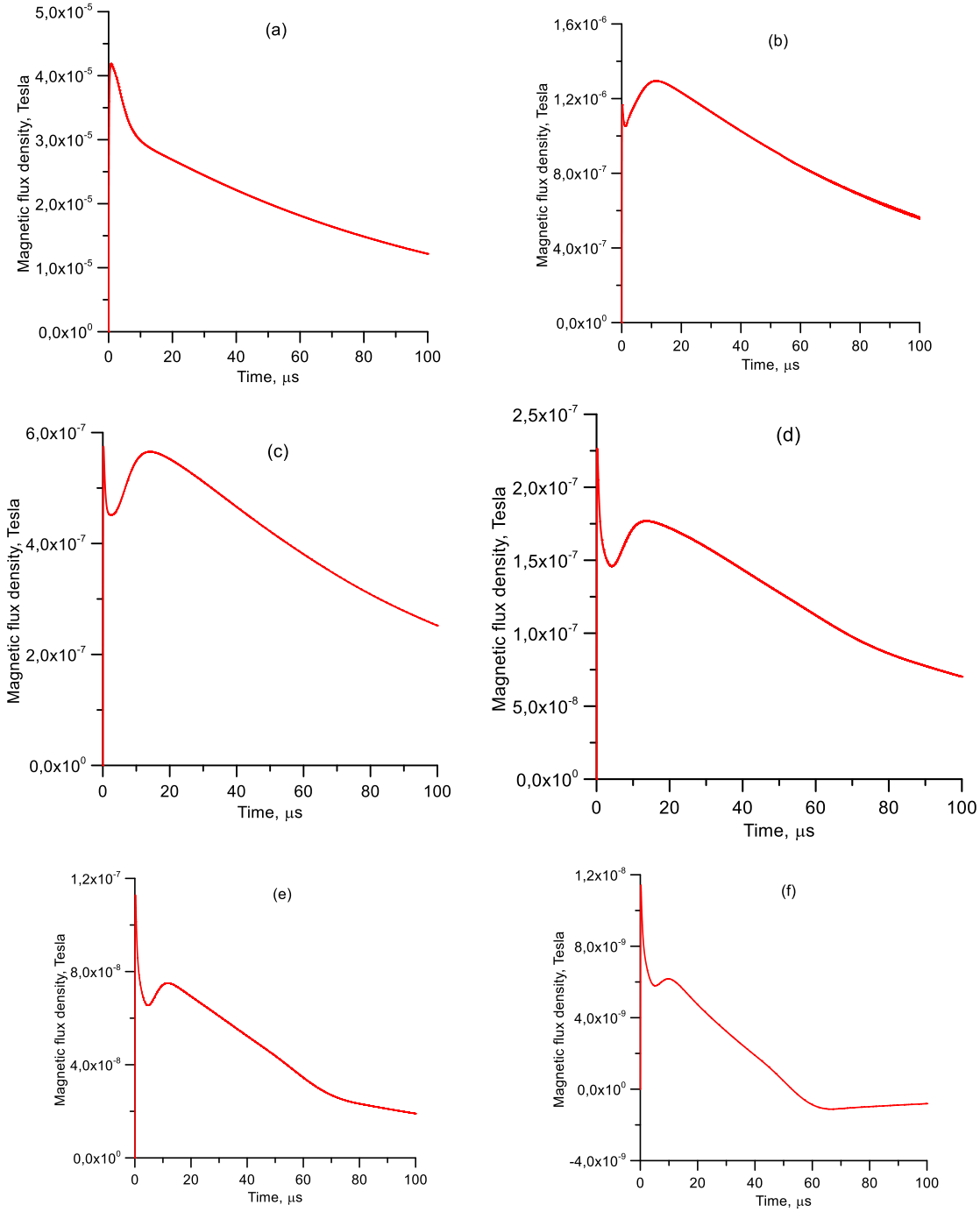

Figure 9. Magnetic field of subsequent return strokes at different distances as predicted by the MTLD model that incorporates current dispersion. (**a**) 50 m, (**b**) 1 km, (**c**) 2 km, (**d**) 5 km, (**e**) 10 km and (**f**) 100 km. The return stroke speed is assumed to be constant and equal to 1.5×10^8 m/s.

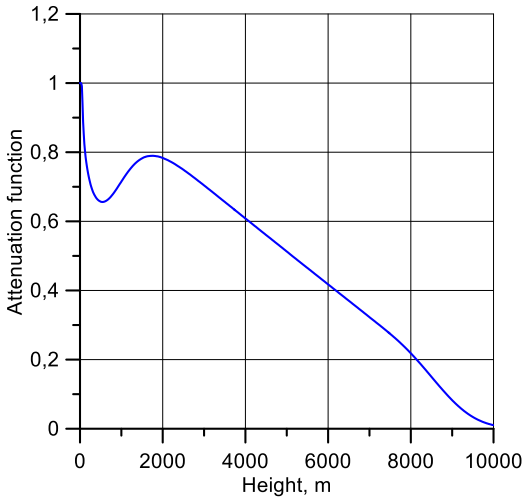

Figure 10. Attenuation function derived from the radiation field depicted by curve 1 in Figure 7 using Equation (12), assuming that the channel base current propagates upwards without dispersion.

Now, the reader might wonder whether the inversion formula we have derived earlier, i.e., Equation (12), is compatible with the MTLD model which incorporates current dispersion. Actually, one can use this equation to extract the current attenuation curve in the presence of dispersion. The only change needed is to replace the derivative of the current at any height in Equation (12) by the derivative of the dispersed current at that height. The current waveform at any height with dispersion can be easily obtained from the convolution integral as we have explained earlier.

7. MTLD Model—First Return Strokes

The current attenuation function extracted for the subsequent return strokes is also used to evaluate the electromagnetic fields of first return strokes. We believe that this attenuation function is also valid for first return strokes if one neglects the effects of branches. In this exercise, the channel base current was replaced by the one corresponding to the first return strokes and the uniform return stroke speed was reduced from 1.5×10^8 m/s to 1.0×10^8 m/s. Our calculations show that the zero-crossing time of the resulting radiation field is about 60–70 μs, whereas the measured zero-crossing time of the radiation fields in the tropics is about 94 μs. We believe that the reason for this discrepancy in the zero-crossing time is the assumed uniformity of the return stroke speed. As discussed earlier, in general, the return stroke speed decreases with height and this decrease is more significant in the case of first return strokes. For example, according to Schonland [27], the first return stroke speed close to the channel base is typically near 10^8 m/s and the speed at the top of the channel is typically around 0.5×10^8 m/s. For this reason, we have incorporated a return stroke speed profile that decreases exponentially with height (denoted by the decay height constant λ_v) into our calculation. Observe that a decreasing return stroke speed with height will give rise to a longer zero-crossing time compared to the value pertinent to a uniform speed. Since we are applying the model to reproduce fields in tropical regions, we changed the value of λ_v until the zero-crossing time of the radiation field reached around 90 μs.

The electric and magnetic fields calculated at different distances for first return strokes using the attenuation function and the exponentially decreasing velocity profile are shown in Figures 11 and 12, respectively. Since the current dispersion is a feature that is present both in subsequent and first return strokes [33,34], we have included the same dispersion function used for subsequent return strokes in the calculations. For comparison purposes, the waveforms predicted by the MTLE and MTLL models for the first return stroke are also given in the same diagrams.

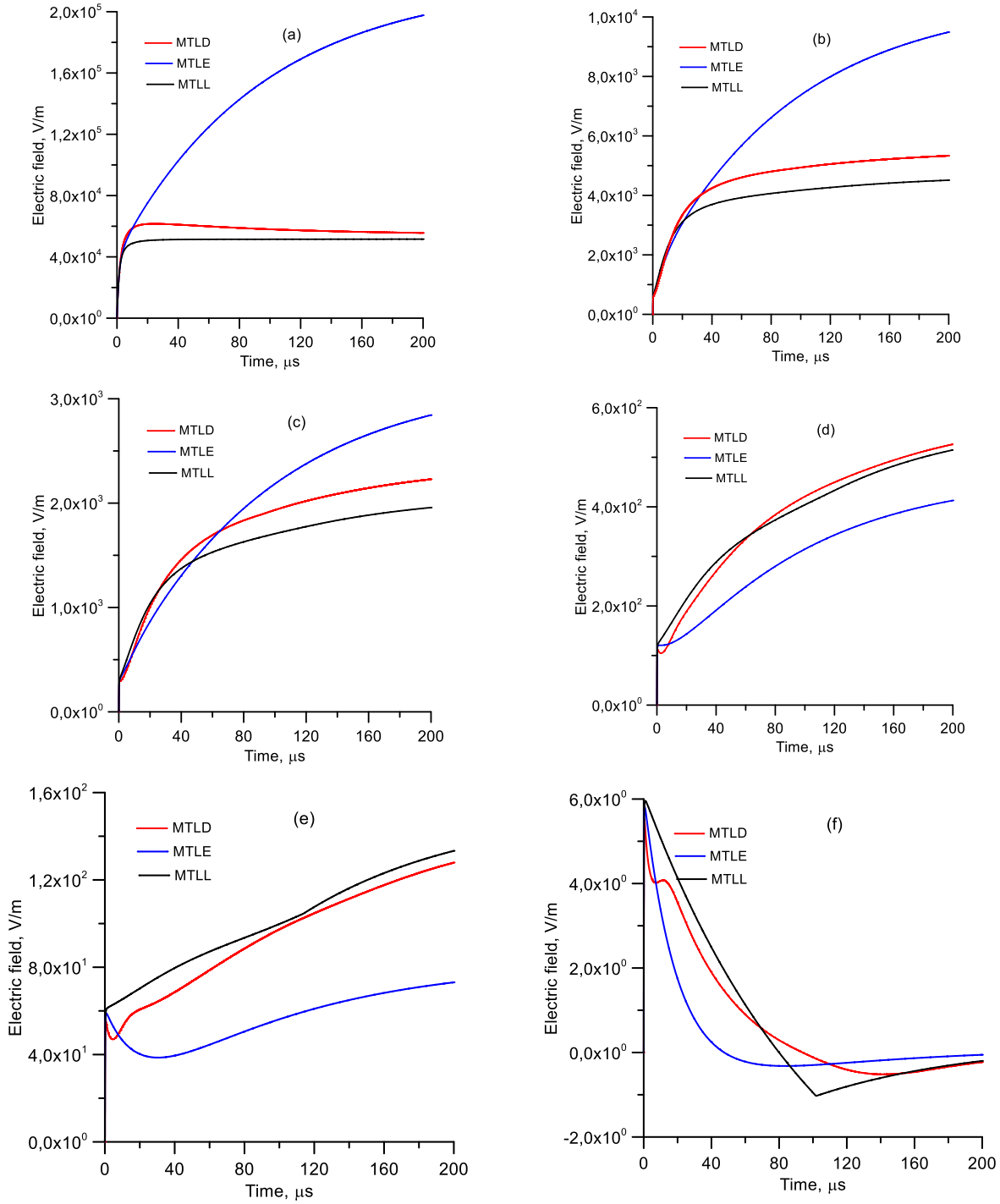

Figure 11. Electric field of first return strokes at different distances as predicted by the MTLD (with dispersion and decreasing velocity profile with λ_v = 10 km), MTLE and MTLL models. (**a**) 50 m, (**b**) 1 km, (**c**) 2 km, (**d**) 5 km, (**e**) 10 km and (**f**) 100 km. In the MTLE model, λ = 2.0 km and, in the MTLL model, H = 10 km are used as model parameters. In the MTLE and MTLL models, the return stroke speed remains constant at 1.0×10^8 m/s.

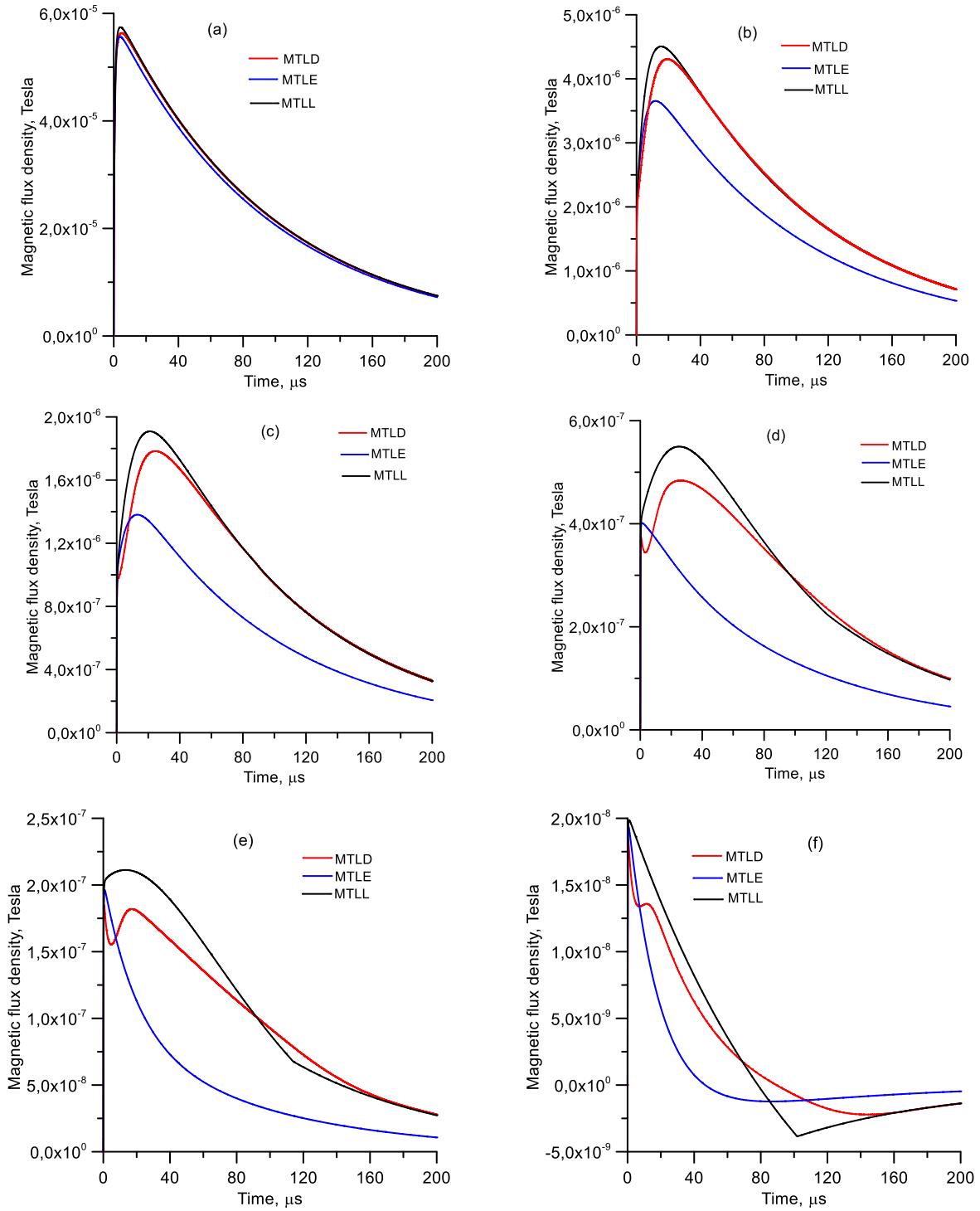

Figure 12. Magnetic field of first return strokes at different distances as predicted by the MTLD (with dispersion and decreasing velocity profile with λ_v = 10 km), MTLE and MTLL models. (**a**) 50 m, (**b**) 1 km, (**c**) 2 km, (**d**) 5 km, (**e**) 10 km and (**f**) 100 km. In the MTLE model, λ = 2.0 km and, in the MTLL model, H = 10 km are used as model parameters. In the MTLE and MTLL models, the return stroke speed remains constant at 1.0×10^8 m/s.

Note that the calculated fields are similar to the typical first return stroke fields reported by Lin et al. [24]. The electric fields around 1 km to 10 km display a ramp-like increase and the distant radiation field crosses the zero line. The close magnetic fields display the characteristic hump. As in the case of subsequent return strokes, the electric field in the vicinity of the channel almost saturates within a few tens of microseconds.

8. Input Parameters of the MTLD Model

As mentioned earlier, the derived attenuation function depends on the shape and the zero-crossing time of the radiation field. In particular, the height at which the current attenuation function goes to zero depends mainly on the zero-crossing time of the radiation field. As we have seen earlier, the derived attenuation function, which is based on radiation fields from the tropics, goes to zero at channel heights around 10 km.

The derived attenuation function can be approximated as a function of height z along the channel by the following polynomial expressions (polynomial fits to the derived attenuation function were obtained using a standard plotting program):

$$A = \sum_{n=1}^{9} A_n z^{n-1} \quad z \leq 10000 \tag{19}$$

The coefficients of the polynomials are the following: $A_1 = 1.00014$, $A_2 = -6.447 \times 10^{-5}$, $A_3 = -1.1292 \times 10^{-7}$, $A_4 = 8.6666 \times 10^{-11}$, $A_5 = -3.3247 \times 10^{-14}$, $A_6 = 7.1764 \times 10^{-18}$, $A_7 = -8.7659 \times 10^{-22}$, $A_8 = 5.6148 \times 10^{-26}$, $A_9 = -1.4580 \times 10^{-30}$.

Our analysis shows that this attenuation function can also be represented by the following equation.

$$A = 0.05 \exp(-z/1000) + 0.95(1.0 - \frac{z}{9600} + \frac{ze^{-z/500}}{9600}) \text{ for } z \leq 5600.0 \tag{20}$$

$$A = \left\{ 0.05 \exp(-z/1000) + 0.95(1.0 - \frac{z}{9600} + \frac{ze^{-z/500}}{9600}) \right\} e^{-\{(z-5600)/3.2\times 10^3\}^3} \text{ for } 5600 < z \leq 9600 \tag{21}$$

Assuming that the spatial variation of the charge distributions at the channel end does not change significantly when the channel height is changed, the above equation can be generalized to any channel height, H, by the following equation

$$A = a\mathrm{e}^{-z/\lambda_1} + (1-a)(1.0 - \frac{z}{H} + \frac{ze^{-z/\lambda_2}}{H}) \text{ for } z \leq H - s \tag{22}$$

$$A = \left\{ a\mathrm{e}^{-z/\lambda_1} + (1-a)(1.0 - \frac{z}{H} + \frac{ze^{-z/\lambda_2}}{H}) \right\} e^{-(z+s-H)^3/\lambda_3^3} \text{ for } H - s < z \leq H \tag{23}$$

In the above expression, $a = 0.05$, $\lambda_1 = 1$ km, $\lambda_2 = 500$ m, $\lambda_3 = 3.2$ km, $s = 0.58\ H$ and H is the height of the channel. This represents the attenuation function corresponding to the MTLD model. It is pleasing to see that, except for the differences at the upper end of the channel, the attenuation function has features similar to those of the the MTLE and MTLL model. For example, it will reduce to the MTLE model when $a = 1$ and to the MTLL model when $a = 0$ and $\lambda_2 = 0$. As the parameters of Equations (22) and (23) vary, the model will give rise to a variety of shapes for the electromagnetic fields and we expect that the above expressions would be able to match the attenuation function corresponding to a variety of electromagnetic fields. Recall again that the attenuation function will change as the waveshape of the radiation field is modified.

In the MTL type models, the charge deposited along the leader channel by the return stroke depends on the attenuation function. The charge deposited along the leader channel for the attenuation function given by Equations (20) and (21) is depicted in Figure 13 together with the charge distributions pertinent to the MTLL and MTLE models. Observe the differences in the charge distributions predicted by the three models. It is of interest to point out that the shape of the distribution of the charge deposited along the channel by the return stroke can be directly connected to the various parameters of Equations (22) and (23). The value of λ_2 decides the risetime of the charge distribution and the value of the initial peak of the charge distribution is controlled by λ_1. As λ_2 increases, the peak of the charge distribution is pushed upwards and this will control how fast the close electric field

saturates (Figure 11a). It also controls how fast the steady value of the charge is reached. The steady value of the charge distribution is controlled by H. As H increases, the steady value decreases. The peak at the tail of the charge distribution and how the charge will go to zero at the channel end is decided by λ_3. Together with H, it controls the zero-crossing time of the distant field (Figures 11f and 12f) for a given return stroke speed.

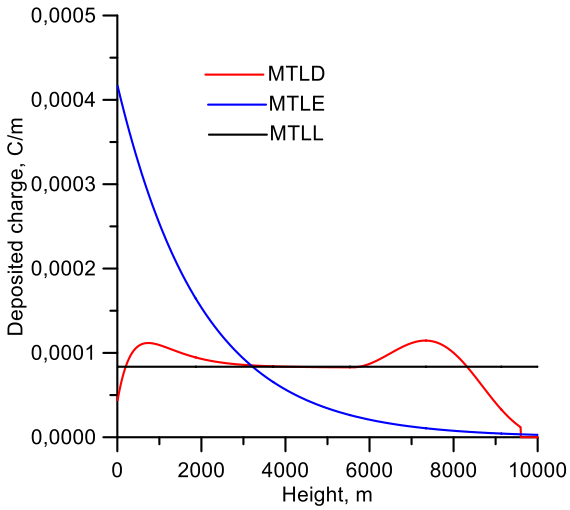

Figure 13. Charge deposited by the return stroke along the leader channel by the MTLD, MTLE and MTLL models. In the MTLE model, $\lambda = 2$ km and, in the MTLL model, $H = 10$ km.

These expressions for the attenuation functions, together with the current dispersion defined by Equations (17) and (18) with $t_0 = 2.5$ μs and $\lambda_r = 500$ m, represent the model parameters necessary to define the attenuation and dispersion of the return stroke current and the resulting electromagnetic fields from first and subsequent strokes in different geographical regions. Typical fields are obtained when the speed of the subsequent return stroke is kept around 1.5×10^8 m/s and when the corresponding speed of first return strokes is defined by $v = v_0 e^{-z/\lambda_v}$ with $v_0 = 10^8$ m/s and $\lambda_v = 10$ km. Unfortunately, the introduction of current dispersion into the MTLD model will increase the complexity of the model, which could be a drawback if the goal is to obtain the electromagnetic fields at different distances for engineering studies. We have investigated whether there is a way to obtain fields similar to those of the MTLD model that include current dispersion, namely, featuring a subsidiary peak, with a simple MTL-type model where the input parameters are the channel base current, return stroke speed and the current attenuation. This could be realized if we change the channel base current waveforms slightly to include a subsidiary peak in them. For example, the first and subsequent return stroke current waveforms shown in Figure 14 together with the current attenuation functions given previously will be able to generate electromagnetic fields similar to those obtained experimentally, even without the current dispersion. These current waveforms can be described analytically by the expression given by Equation (15) with the following parameters: $i_{01} = 14.255$ kA, $i_{02} = 9.36$ kA, $\tau_{11} = 0.055$ μs, $\tau_{12} = 1.92$ μs, $\tau_{21} = 3.6$ μs and $\tau_{22} = 100$ μs for subsequent return strokes and $i_{01} = 34.085$ kA, $i_{02} = 34.8$ kA, $\tau_{11} = 0.1$ μs, $\tau_{12} = 5.0$ μs, $\tau_{21} = 5.0$ μs and $\tau_{22} = 90$ μs for first return strokes.

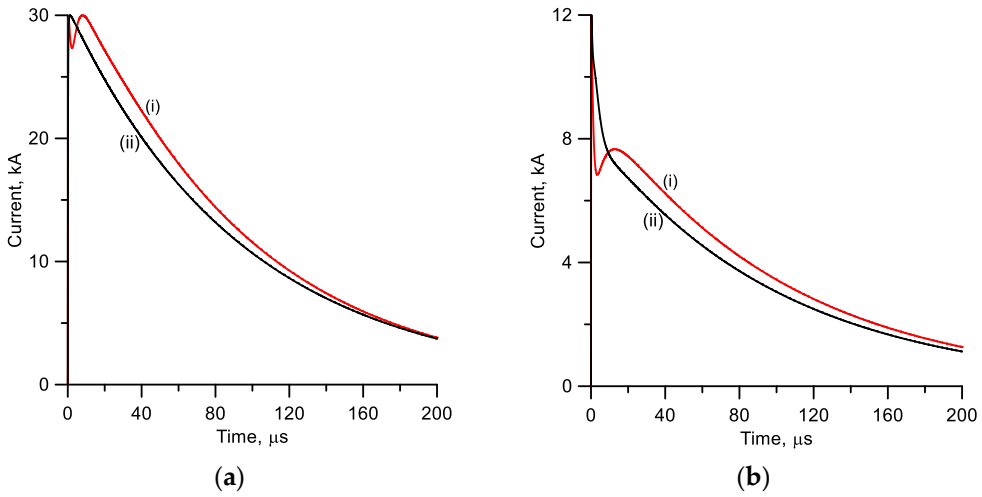

Figure 14. Alternative current waveforms (curves marked (i)) (**a**) for first return strokes and (**b**) for subsequent return strokes that could be used with the MTLD model without current dispersion to generate electromagnetic fields similar to those observed in practice. The curves marked (ii) are the standard current waveforms used in the calculations.

Observe that both the first and the subsequent return stroke currents contain a subsidiary peak. As mentioned earlier, subsidiary peaks such as the one shown in Figure 14b are occasionally observed in triggered lightning but whether this is a more frequent feature in the natural subsequent return stroke currents is a question that needs further investigation [25,26]. On the other hand, return stroke currents observed in tower measurements show a subsidiary peak similar to the first return stroke current shown in Figure 14a (see [37,38] for first strokes in downward negative flashes and [39] for subsequent strokes in upward negative flashes). The reason why some of the current waveforms display a subsidiary peak while others do not have this feature is not known at present. As we have pointed out earlier, for a given radiation field, the features of the derived attenuation function depend on the temporal variation of the channel base current. This calls for further investigations on the connection between the features of the channel base current, attenuation function and the distant radiation fields. More experimental data on the channel base currents and distant radiation fields of return strokes could help us in answering some of these questions.

9. Discussion

The main goal of this paper is to illustrate how the current attenuation function pertinent to MTL-type models could be extracted from the radiation field given the channel base current and the return stroke speed. The extracted current attenuation function depends on the spatial variation of the return stroke speed and the temporal features of the radiation field and the channel base current. Even though we have presented a typical set of parameters for the MTLD model that could be used in engineering applications, it is important to point out that MTLD model is a dynamic model with model parameters changing with the features of the radiation field and the channel base current. The model could easily be tested if the channel base current and the electric fields at two distances, one close to the strike point and the other at a distance where the radiation field dominates, are measured. Even in the case where the channel base current is not known, the model could still be validated by using the two field measurements in combination with a typical channel base current and return stroke speed. The procedure should work without difficulties in the case of subsequent return strokes where the return stroke channel is free from branches. In this case, the changes in the radiation field are either caused by the changes in the return stroke speed, current attenuation or current dispersion, the features of which are already included in the model. However, in the case of first return strokes, the changes in the return stroke current caused by channel branches could modify the radiation field and

these modifications could not be accommodated within the MTLD model, which assumes the return stroke channel to be straight and free from branches. Thus, in the case of first return stroke fields, one has to utilize waveshapes that represent the average temporal behavior of the radiation field that averages out the peaks and dips in the radiation field.

The risetime of the first and subsequent return stroke current waveforms used in the current study are smaller than the risetime of the current waveforms used in reference [19] where Equation (16) for the standard current waveforms is defined. The reason for this difference is the following. The experimental data show that the time of the radiation field range normalized to 100 km is about 30–50 V/m/μs for both first and subsequent return strokes [40,41]. The standard current waveforms, as defined in [20], generate radiation field derivatives that are significantly lower than these experimentally observed values. The changes in the risetime of the current waveforms were made to generate electric field derivatives that are within the ballpark of the experimental observations. Of course, we are aware that the risetimes of the measured current waveforms, especially the ones pertinent to first return strokes, are longer than the ones associated with the current waveforms used in this study. However, it is possible that, due to the physical scenario associated with the lightning attachment process, the channel base current does not show the true risetime of the return stroke current waveform that led to the high electric field derivatives. For example, the risetime of the current waveform at the point of initiation of the return stroke where the upward connecting leader is met with the downward stepped leader could be much smaller than the current waveform at the channel base, which is somewhat distorted by the presence of the connecting leader [42]. Since the MTLD model is based on the features of the radiation field, it is important at this stage to have these features be as accurate as possible even though this may require a slight modification of the current waveform that is frequently used as a standard in the calculation of electromagnetic fields. However, more experimental studies are required to understand how the fast derivatives and the subsidiary peaks in the radiation fields are generated and what is the contribution of the channel base current to these features. As our understanding of the initial stages of the return stroke grows with such studies, we will be able to redefine the parameters of the engineering models.

In this paper, we have used the simplest form of current propagation type models, namely, the modified transmission line model (MTL model), to extract the current attenuation function given the distant radiation field. In the MTL-type models, the attenuation function at any height is time independent since the currents are only scaled by a constant factor when the return stroke propagates from one height to another. Because of this feature, the total deposited charge at any height depends only on the height and not time [43] and the time dependence of the charge deposition (i.e., corona current) does not depend on the height. Moreover, the charge deposition at any given height takes place over the whole duration of the return stroke current. That is, the duration of the corona current neutralizing the leader corona sheath is equal to the duration of the return stroke current. However, the duration of the corona current could be shorter than the duration of the return stroke current. If this is the case, it will lead to a current attenuation function that depends on time. That is, at any given height, the current is attenuated by different amounts at different times. One way to incorporate this feature into the MTL-type models is to allow the current dispersion process to deposit charge along the return stroke channel and describe the current attenuation purely based on a current dispersion process. This point is under investigation at present. On the other hand, a time-dependent current attenuation is a feature that is present in the current generation-type return stroke models. Indeed, the inverse procedure that we have described in this paper can be done with the simplest form of current generation-type model, where the third input parameter is the variation of the corona current with height [7]. This point too is under investigation at present.

10. Conclusions

In this paper, we have shown that within the assumption of MTL-type models, i.e., models in which the return stroke current pulse injected at the channel base propagates up along the channel with attenuation but without distortion, one can extract the current attenuation function from the measured radiation fields. In this inverse process, it is assumed that both the channel base current and the return stroke velocity are measured and could be used as inputs. It was shown using the MTLE and MTLL models that the inverse procedure works correctly once the above inputs are available. Using the radiation fields with features similar to those of subsequent return strokes, the current attenuation function pertinent to return strokes was estimated. The extracted attenuation function in turn was used in an MTL-type model, named the MTLD model, to calculate the electromagnetic fields at different distances. The results were compared with calculations based on the MTLL and MTLE models. It was shown that in order to generate electromagnetic fields similar to those observed experimentally, it is necessary to include current dispersion and, in the case of first return strokes, a reduction of return stroke speed with height. The features of the electromagnetic fields thus obtained using the MTLD model are in general agreement with measurements at all distances.

Author Contributions: V.C. conceived the idea and developed analytical procedures. All authors contributed equally in the analysis and in writing the paper. All authors have read and agreed to the published version of the manuscript.

Funding: This research received no external funding.

Institutional Review Board Statement: Not applicable.

Informed Consent Statement: Not applicable.

Data Availability Statement: Not applicable.

Acknowledgments: The work presented here is supported by Svea Andersson donation at the Division for Electricity, Department of Electrical Engineering, Uppsala University, Sweden. First author thanks Mats Leijon for placing research facilities at his disposal.

Conflicts of Interest: The authors declare no conflict of interest.

References

1. Boccippio, D.J.; Williams, E.R.; Heckman, S.J.; Lyons, W.A.; Baker, I.T.; Boldi, R. Sprites, ELF Transients, and Positive Ground Strokes. *Science* **1995**, *269*, 1088–1091. [CrossRef] [PubMed]
2. Rachidi, F.; Nucci, C.A.; Ianoz, M. Transient Analysis of Multiconductor Lines Above a Lossy Ground. *IEEE Trans. Power Deliv.* **1999**, *14*, 294–302. [CrossRef]
3. Nucci, C.A.; Rachidi, F.; Ianoz, M.V.; Mazzetti, C. Influence of a Lossy Ground on Lightning Induced Voltages on Overhead Lines. *IEEE Trans. Electromagn. Compat.* **1993**, *35*, 75–86. [CrossRef]
4. Ye, M.; Cooray, V. Propagation Effects Caused by a Rough Ocean Surface on the Electromagnetic Fields Generated by Lightning Return Strokes. *Radio Sci.* **1994**, *29*, 73–85.
5. Cooray, V.; Ye, M. Propagation Effects on the Lightning-Generated Electromagnetic Fields for Homogeneous and Mixed Sea Land Paths. *J. Geophys. Res.* **1994**, *99*, 10641–10652. [CrossRef]
6. Cooray, V. On the Various Approximations to Calculate Lightning Return Stroke Generated Electric and Magnetic Fields Over Finitely Conducting Ground. In *Lightning Electromagnetics*; Cooray, V., Ed.; IET: Stevenage, UK, 2012.
7. Cooray, V. Lightning Return Stroke Models for Electromagnetic Field Calculations. In *Lightning Interaction with Power Systems*; Piantini, A., Ed.; IET Publishers: London, UK, 2020; Volume 1.
8. Uman, M.A.; McLain, D.K. Magnetic Field of Lightning Return Stroke. *J. Geophys. Res.* **1969**, *74*, 6899–6910. [CrossRef]
9. Nucci, C.A.; Mazzetti, C.; Rachidi, F.; Ianoz, M. On Lightning Return Stroke Models for Lemp Calculations. In Proceedings of the 19th International Conference Lightning Protection, Graz, Austria, 25–28 April 1988.
10. Rakov, V.A.; Dulzon, A.A. A Modified Transmission Line Model for Lightning Return Stroke Field Calculation. In Proceedings of the 9th International Symposium on Electromagnetic Compatibility, Zurich, Switzerland, 12–14 March 1991; pp. 229–235.
11. Rachidi, F.; Nucci, C.A. On the Master, Lin, Uman, Standler and the Modified Transmission Line Lightning Return Stroke Current Models. *J. Geophys. Res.* **1990**, *95*, 20389–20394. [CrossRef]
12. Javor, V. Modified Transmission Line Models of Lightning Strokes Using New Current Functions and Attenuation Factors. In *Engineering Mathematics I*; Springer: Cham, Switzerland, 2016; pp. 131–149.

13. Feynman, R. *The Character of Physical Law*; The Modern Library: New York, NY, USA, 1994.
14. Rachidi, F.; Thottappillil, R. Determination of Lightning Currents from Far Electromagnetic Fields. *J. Geophys. Res.* **1993**, *98*, 18315–18321. [CrossRef]
15. Delfino, F.; Procopio, R.; Andreotti, A.; Verolino, L. Lightning Return Stroke Current Identification via Field Measurements. *Electr. Eng.* **2002**, *84*, 41–50. [CrossRef]
16. Andreotti, A.; De Martinis, U.; Verolino, L. An Inverse Procedure for the Return Stroke Current Identification. *IEEE Trans. Electromagn. Compat.* **2001**, *43*, 155–160. [CrossRef]
17. Willett, J.C.; Le Vine, D.M.; Idone, V.P. Lightning Return Stroke Current Waveforms Aloft from Measured Field Change, Current, And Channel Geometry. *J. Geophys. Res. Atmos.* **2008**, *113*. [CrossRef]
18. Izadi, M.; Ab Kadir, M.Z.A.; Askari, M.T.; Hajikhani, M. Evaluation of Lightning Current Using Inverse Procedure Algorithm. *Int. J. Appl. Electromagn. Mech.* **2013**, *41*, 267–278. [CrossRef]
19. Cooray, V.; Cooray, G. A Novel Interpretation of the Electromagnetic Fields of Lightning Return Strokes. *Atmosphere* **2019**, *10*, 22. [CrossRef]
20. Delfino, F.; Procopio, R.; Rossi, M.; Rachidi, F.; Nucci, C.A. An Algorithm for the Exact Evaluation of The Underground Lightning Electromagnetic Fields. *IEEE Trans. EMC* **2007**, *49*, 401–411. [CrossRef]
21. Cooray, G.V. Remote Sensing of Lightning Return Strokes through the Electric Radiation Fields. Ph.D. Thesis, Uppsala University, Uppsala, Sweden, 1982.
22. Cooray, V.; Lundquist, S. Characteristics of the Radiation Fields from Lightning in Sri Lanka in the Tropics. *J. Geophys. Res.* **1985**, *90*, 6099–6109. [CrossRef]
23. Weidman, C.D.; Krider, E.P. The Fine Structure of Lightning Return Stroke Wave Forms. *J. Geophys. Res. Lett.* **1980**, *7*, 955–958. [CrossRef]
24. Lin, Y.T.; Uman, M.A.; Tiller, J.A.; Brantley, R.D.; Beasley, W.H.; Krider, E.P.; Weidman, E.D. Characterization of Lightning Return Stroke Electric and Magnetic Fields from Simultaneous Two-Station Measurements. *J. Geophys. Res.* **1979**, *84*, 6307–6314. [CrossRef]
25. Schnetzer, G.H.; Fisher, R.J.; Rambo, K.J. *1996 Joint Sandia/University of Florida Triggered Lightning Test Program: Temporary Lightning Protection System Experiments and Direct Strikes to Explosive Materials*; Department of Electrical and Computer Engineering, University of Florida: Gainesville, FL, USA, 1996.
26. Fisher, R.J.; Schnetzer, G.H. *1993 Triggered Lightning Test Program: Environment Within 20 Meters of the Lightning Channel and Small Area Temporary Protection Concepts*; Sandia Report, Sand94-0311, UC-706; Sandia National Laboratories: Albuquerque, NM, USA, 1994.
27. Schonland, B.F.J. The Lightning Discharge. In *Handbuch Der Physik*; Springer: Heidelberg/Berlin, Germany, 1956; Volume 22, pp. 576–628.
28. Cooray, V.; Orville, R.E. The Effects of Variation of Current Amplitude, Current Risetime and Return Stroke Velocity along the Return Stroke Channel on the Electromagnetic Fields Generated by Return Strokes. *J. Geophys. Res.* **1990**, *95*, D11. [CrossRef]
29. Gorin, B.N. Mathematical Modeling of the Lightning Return Stroke. *Elektrichestvo* **1985**, *4*, 10–16.
30. Srivastava, K.M.L. Return Stroke Velocity of a Lightning Discharge. *J. Geophys. Res.* **1966**, *71*, 1283–1286. [CrossRef]
31. Olsen, R.C.; Jordan, D.M.; Rakov, V.A.; Uman, M.A.; Grimes, N. Observed Two-Dimensional Return Stroke Propagation Speeds in The Bottom 170 M of a Rocket-Triggered Lightning Channel. *Geophys. Res. Lett.* **2004**, *31*, L16107. [CrossRef]
32. Wait, J.R. On the Electromagnetic Pulse Response of a Dipole over a Plane Surface. *Can. J. Phys.* **1974**, *52*, 153–196. [CrossRef]
33. Jordan, D.M.; Uman, M.A. Variation in Light Intensity with and Time from Subsequent Lightning Return Strokes. *J. Geophys. Res.* **1983**, *88*, 6555–6562. [CrossRef]
34. Mach, D.M.; Rust, W.D. Photoelectric Return Stroke Velocity and Peak Current Estimates in Natural and Triggered Lightning. *J. Geophys. Res.* **1989**, *94*, 13237–13247. [CrossRef]
35. Gomes, C.; Cooray, V. Correlation between the Optical Signatures and Current Wave Forms of Long Sparks: Applications in Lightning Research. *J. Electrost.* **1998**, *43*, 267–274. [CrossRef]
36. Jordan, D.M.; Idone, V.P.; Orville, R.E.; Rakov, V.A.; Uman, M.A. Luminosity Characteristics of Lightning M Components. *J. Geophys. Res.* **1995**, *100*, 25695–25700. [CrossRef]
37. Berger, K. Novel Observations of Lightning Discharges: Results of Research on Mount San Salvatore. *J. Frankl. Inst.* **1967**, *283*, 478–525. [CrossRef]
38. Visacro, S.; Mesquita, C.R.; De Conti, A.; Silveira, F.H. Updated Statistics of Lightning Currents Measured at Morro Do Cachimbo Station. *Atmos. Res.* **2012**, *117*, 55–63. [CrossRef]
39. Li, D.; Azadifar, M.; Rachidi, F.; Rubinstein, M.; Paolone, M.; Pavanello, D.; Metz, S.; Zhang, Q.; Wang, Z. On Lightning Electromagnetic Field Propagation along an Irregular Terrain. *IEEE Trans. Electromagn. Compat.* **2016**, *58*, 161–171. [CrossRef]
40. Willett, J.; Krider, E.; Leteinturier, C. Submicrosecond Field Variations during the Onset of First Return Strokes in Cloud-to-Ground Lightning. *J. Geophys. Res.* **1996**, *103*, 9027–9034. [CrossRef]
41. Le Vine, D.M.; Willett, J.C.; Bailey, J.C. Comparison of Fast Electric Field Changes from Subsequent Return Strokes of Natural and Triggered Lightning. *J. Geophys. Res.* **1989**, *94*, 13259–13265. [CrossRef]
42. Cooray, V. A Model for Negative First Return Strokes in Negative Lightning Flashes. *Phys. Scrip.* **1997**, *55*, 119–128. [CrossRef]
43. Thottappillil, R.; Rakov, V.A.; Uman, M.A. Distribution of Charge along the Lightning Channel: Relation to Remote Electric and Magnetic Fields and to Return-Stroke Models. *J. Geophys. Res.* **1997**, *102*, 6987–7006. [CrossRef]